

UNCLASSIFIED

AD NUMBER

AD914659

LIMITATION CHANGES

TO:

Approved for public release; distribution is unlimited.

FROM:

Distribution authorized to U.S. Gov't. agencies only; Test and Evaluation; NOV 1973. Other requests shall be referred to Air Force Flight Dynamics Laboratory, Attn: FER, Wright-Patterson, AFB 45433.

AUTHORITY

AFWAL ltr, 6 Nov 1980

THIS PAGE IS UNCLASSIFIED

cy 3



EFFECT OF A HIGH STRENGTH-TO-WEIGHT RATIO MATERIAL ON PARACHUTE PERFORMANCE AT MACH NUMBER 0.8

W. L. Peters
ARO, Inc.

PROPULSION WIND TUNNEL FACILITY
ARNOLD ENGINEERING DEVELOPMENT CENTER
AIR FORCE SYSTEMS COMMAND
ARNOLD AIR FORCE STATION, TENNESSEE 37389

November 1973

Final Report for Period 26-27 July, 1973

Per TAB No. 81-2.

Distribution limited to U. S. Government agencies only; this report contains information on test and evaluation of military hardware; November 1973; other requests for this document must be referred to Air Force Flight Dynamics Laboratory (FER), Wright-Patterson AFB, OH 45433.

Prepared for

AIR FORCE FLIGHT DYNAMICS LABORATORY (FER)
WRIGHT-PATTERSON AFB, OH 45433

NOTICES

When U. S. Government drawings specifications, or other data are used for any purpose other than a definitely related Government procurement operation, the Government thereby incurs no responsibility nor any obligation whatsoever, and the fact that the Government may have formulated, furnished, or in any way supplied the said drawings, specifications, or other data, is not to be regarded by implication or otherwise, or in any manner licensing the holder or any other person or corporation, or conveying any rights or permission to manufacture, use, or sell any patented invention that may in any way be related thereto.

Qualified users may obtain copies of this report from the Defense Documentation Center.

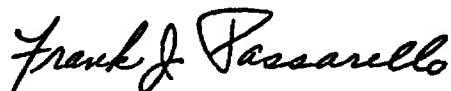
References to named commercial products in this report are not to be considered in any sense as an endorsement of the product by the United States Air Force or the Government.

APPROVAL STATEMENT

This technical report has been reviewed and is approved.



LAMAR R. KISSLING
Lt Colonel, USAF
Chief Air Force Test Director, PWT
Directorate of Test



FRANK J. PASSARELLO
Colonel, USAF
Director of Test

UNCLASSIFIED

SECURITY CLASSIFICATION OF THIS PAGE (When Data Entered)

REPORT DOCUMENTATION PAGE		READ INSTRUCTIONS BEFORE COMPLETING FORM
1. REPORT NUMBER AEDC-TR-73-184	2. GOVT ACCESSION NO.	3. RECIPIENT'S CATALOG NUMBER
4. TITLE (and Subtitle) EFFECT OF A HIGH STRENGTH-TO-WEIGHT RATIO MATERIAL ON PARACHUTE PERFORMANCE AT MACH NUMBER 0.8		5. TYPE OF REPORT & PERIOD COVERED Final Report - July 26 to 27, 1973
7. AUTHOR(s) W. L. Peters, ARO, Inc.		6. PERFORMING ORG. REPORT NUMBER ARO-PWT-TR-73-128
9. PERFORMING ORGANIZATION NAME AND ADDRESS Arnold Engineering Development Center (XO) Arnold Air Force Station, Tennessee 37389		8. CONTRACT OR GRANT NUMBER(s)
11. CONTROLLING OFFICE NAME AND ADDRESS Air Force Flight Dynamics Laboratory (FER), Wright-Patterson AFB, OH 45433		10. PROGRAM ELEMENT, PROJECT, TASK AREA & WORK UNIT NUMBERS Program Element 62201F Project 6065
14. MONITORING AGENCY NAME & ADDRESS (if different from Controlling Office)		12. REPORT DATE November 1973
		13. NUMBER OF PAGES 30
		15. SECURITY CLASS. (of this report) UNCLASSIFIED
		15a. DECLASSIFICATION/DOWNGRADING SCHEDULE N/A
16. DISTRIBUTION STATEMENT (of this Report) Distribution limited to U. S. Government agencies only; this report contains information on test and evaluation of military hardware; November 1973; other requests for this document must be referred to Air Force Flight Dynamics Laboratory (FER), Wright-Patterson AFB, OH 45433.		
17. DISTRIBUTION STATEMENT (of the abstract entered in Block 20, if different from Report)		
18. SUPPLEMENTARY NOTES Available in DDC.		
19. KEY WORDS (Continue on reverse side if necessary and identify by block number) parachute fabrics transonic flow drag chutes drag ribbon parachutes		
20. ABSTRACT (Continue on reverse side if necessary and identify by block number) Tests were conducted in the AEDC Propulsion Wind Tunnel (16T) to determine the deployment and inflation characteristics of five conical ribbon parachute configurations with individual parachute components (suspension lines, radials, and canopy ribbons) in each configuration constructed with nylon material or a new textile material, Fiber B. Dynamic deployment data were obtained at a		

UNCLASSIFIED

SECURITY CLASSIFICATION OF THIS PAGE(When Data Entered)

20, Continued

nominal Mach number of 0.8 and dynamic pressures of 350 to 530 psf, and steady-state data were obtained at Mach numbers from 0.6 to 1.3 and a dynamic pressure of 200 psf. In general, parachutes constructed of Fiber B material withstood the same opening shock loads while exhibiting a shorter damping time for deployment drag loads compared with the nylon-constructed parachutes. A significant drag-to-weight increase and a steady-state drag increase with increasing dynamic pressure resulted from the use of Fiber B material compared to nylon material in parachute construction. The least post-deployment drag dynamics were exhibited by those parachutes which had Fiber B-constructed canopy ribbons and radials.

UNCLASSIFIED

SECURITY CLASSIFICATION OF THIS PAGE(When Data Entered)

PREFACE

The work reported herein was conducted by the Arnold Engineering Development Center (AEDC), Air Force Systems Command (AFSC), at the request of the Air Force Flight Dynamics Laboratory (AFFDL/FER), AFSC, Wright-Patterson Air Force Base, Ohio, for the Goodyear Aerospace Corporation, Akron, Ohio. The results presented were obtained by ARO, Inc. (a subsidiary of Sverdrup & Parcel and Associates, Inc.), contract operator of AEDC, AFSC, Arnold Air Force Station, Tennessee. The work was done under ARO Project No. PA340, and the manuscript was submitted for publication on September 19, 1973.

CONTENTS

	<u>Page</u>
1.0 INTRODUCTION	5
2.0 APPARATUS	
2.1 Test Facility	5
2.2 Test Articles	5
2.3 Instrumentation	6
3.0 PROCEDURE	7
4.0 RESULTS AND DISCUSSION	
4.1 Steady-State Performance	7
4.2 Parachute Dynamic Characteristics	8
5.0 CONCLUDING REMARKS	10
REFERENCES	11

ILLUSTRATIONS

Figure

1. Model Location in Test Section	13
2. Sketch of Model Forebody	14
3. Installation of Model Forebody in Test Section	15
4. Parachute Installation	16
5. Sketch Showing Load Cell Installation	17
6. Sketch of Test Parachute	18
7. Weight Comparison of Parachute Configurations	19
8. Volume Comparison of Parachute Configurations	20
9. Variation of Drag Coefficient with Dynamic Pressure, $M_\infty = 0.8$	21
10. Typical Photographs of Deployment and Inflation of the Parachute Configurations, $M_\infty = 0.8$, $q_\infty = 350$ psf	22
11. Variation of Parachute Drag Coefficient with Mach Number, $q_\infty = 200$ psf	23
12. Drag-to-Weight Ratio of Various Configurations, $M_\infty = 0.8$, $q_\infty = 350$ psf	24
13. Deployment Characteristics of Various Configurations, $M_\infty = 0.8$, $q_\infty = 350$ psf	25
14. Typical Distribution Plot of the Parachute Dynamic Drag Characteristics, $M_\infty = 0.8$, $q_\infty = 440$ psf, Configuration BBB3	26
15. Relative Dynamic Parameter and Standard Deviation for Various Configurations, $M_\infty = 0.8$, $q_\infty = 350$ psf	27

TABLES

1. Parachute Configuration Construction	28
2. Test Summary	28
3. Parachute Statistical Analysis Summary	29
 NOMENCLATURE	 30

1.0 INTRODUCTION

The purpose of this test program was to evaluate a recently developed textile material (Fiber B) that could result in a significant reduction of weight and volume of parachute systems. Tests were conducted to compare deployment and inflation characteristics of conical ribbon parachutes having individual parachute components constructed of Fiber B material or conventional nylon material. Sixteen parachutes were deployed from a strut-mounted cylindrical forebody with a flared base section. Dynamic deployment drag data for all parachutes were obtained at a Mach number of 0.8 and dynamic pressures from 350 to 530 psf. Two parachutes were tested for steady-state drag characteristics at Mach numbers from 0.6 to 1.3 and a dynamic pressure of 200 psf.

2.0 APPARATUS

2.1 TEST FACILITY

The AEDC Propulsion Wind Tunnel (16T) is a closed-circuit, continuous flow wind tunnel capable of operation between Mach numbers 0.20 and 1.60. The tunnel can be operated over a stagnation pressure range from 120 to 4300 psfa, depending on Mach number. The test section stagnation temperature can be controlled through a range of about 80 to 160°F as a function of cooling water temperature. The wind tunnel specific humidity is controlled by removing tunnel air and supplying makeup air from an atmospheric dryer. A more complete description of the wind tunnel and its operating characteristics can be found in Ref. 1.

A sketch showing the model location and strut support arrangement in Tunnel 16T is presented in Fig. 1.

2.2 TEST ARTICLES

2.2.1 Model Forebody and Deployment System

The parachutes were deployed from a strut-mounted forebody during these tests. An ogive nose section is normally used on the forebody; however, when difficulties were encountered in deployment, the nose was removed to use dynamic pressure forces to assist the deployment spring system. A dimensional sketch and a test section installation photograph are presented in Figs. 2 and 3, respectively.

The parachute package was placed in the forebody storage compartment located in the flared base section of the model and was restrained against a spring-loaded plate by four straps. These straps were connected by a pyrotechnic-activated release pin mechanism.

A test section parachute installation photograph is presented in Fig. 4. The riser lines of the parachutes were fastened by two pins to a load cell arrangement located in the model forebody. A sketch of this arrangement is shown in Fig. 5.

2.2.2 Parachute Details

Five basic parachute configurations were tested. The individual parachute components (suspension lines, radials, and canopy ribbons) in each configuration were constructed with either Fiber B material or nylon material. (See Table 1 for identification of the material makeup of each test parachute configuration.)

The sixteen parachutes tested were 20-deg conical ribbon chutes with a geometric porosity of 15 percent. The nominal diameter was 6.4 ft with an inflated diameter of approximately 4.2 ft. Each parachute had 16 gores, 16 suspension lines, and 14 horizontal ribbons with individual suspension line strength of approximately 1500 lb. A sketch showing the common dimensions of all test parachutes is presented in Fig. 6.

All test parachutes were constructed of equal strength. Since Fiber B material has a two-to-one strength-to-weight ratio as compared to nylon material, a weight reduction was realized in those parachutes having components made of Fiber B material, as shown in Fig. 7. A corresponding packed volume saving was achieved for parachutes of Fiber B construction, based on the lighter weight for the same strength and greater density of Fiber B material compared to that of nylon material (specific gravity 1.44 for Fiber B versus 1.14 for nylon). The approximate volume of each test parachute configuration is presented in Fig. 8.

2.3 INSTRUMENTATION

The parachute drag load was measured by a 20,000-lb capacity, dual-element load cell to within an accuracy of ± 4 lbf. The outputs from the load cell were digitized and recorded on magnetic tape for on-line, steady-state data reduction and were recorded by a high-speed digital data recording system at a sampling rate of approximately 2000 samples per second for off-line data reduction of parachute drag dynamics. These outputs were also continuously recorded on direct-writing oscillographs for monitoring of load dynamics.

Five motion-picture cameras and a 70-mm still camera visually documented the test, and television cameras were utilized to monitor the forebody and parachutes during the test.

3.0 PROCEDURE

Before the initiation of the wind tunnel test operation, the parachute package was installed in the forebody storage compartment. After test conditions were achieved, a countdown procedure was used to sequence data acquisition during deployment of the parachute. The deployment procedure consisted of activation of the oscillographs, the high-speed digital recording system, and the motion-picture cameras, followed by the ignition of the pyrotechnic squib which initiated the release pin mechanism to deploy the parachute. After inflation of the chute, steady-state drag loads were acquired by electrically averaging the load cell analog output over an interval of 1 sec.

The steady-state drag data were reduced to coefficient form using a reference area based on the nominal parachute diameter of 6.4 ft and by using the tunnel test dynamic pressure value acquired after inflation of the parachute. Because of the sudden increase in tunnel blockage, the tunnel Mach number and dynamic pressure after inflation of the parachute for each test were approximately 93 percent and 90 percent, respectively, of the values prior to deployment. The post-deployment (approximately 2 sec after deployment) dynamic drag performance parameters, such as standard deviation, average drag coefficient, skewness, and kurtosis were calculated from the data recorded by the high-speed recording system utilizing the statistical analysis program which is outlined in Ref. 2.

A summary of testing is presented in Table 2. The nominal tunnel conditions prior to the time of deployment of the parachutes are listed for all configurations except for those parachutes which deployed prematurely. For those designated parachutes, the tunnel conditions after parachute inflation are listed. Each parachute was deployed at only one test condition. The model forebody angle of attack and angle of sideslip were zero deg at all test conditions.

4.0 RESULTS AND DISCUSSION

4.1 STEADY-STATE PERFORMANCE

The data presented in Fig. 9 show the variation of the steady-state drag coefficient with free-stream dynamic pressure for the individual parachute configurations composed partially or wholly of Fiber B material compared to the all-nylon parachute configuration. These data were obtained by electrically averaging the analog outputs over 1-sec intervals. As shown, an increase in the dynamic pressure had little effect on the drag of the all-nylon parachute configuration, NNN. This same increase in the dynamic pressure resulted in

a small increase in drag for the all-Fiber B parachute configuration, BBB, and for parachute configuration NBB.

In Fig. 9, the NNB, NBB, and BBB parachutes exhibited slightly less drag than the NNN parachute. Because the ratio of elongation-to-break of Fiber B material is from 25 to 33 percent that of nylon material, the NNN parachute had a larger inflated diameter and thus a larger drag coefficient based on the nominal diameter than did the Fiber B parachutes. In general, there was good agreement between the data presented in Fig. 9 and the average steady-state drag coefficient calculated by the statistical analysis program. Two exceptions are the BNN parachute at a dynamic pressure of 318 psf and a drag coefficient value of 0.591 and the NBB parachute at a dynamic pressure of 317 psf and a drag coefficient value of 0.604. Analysis of the motion pictures and the photographs as taken by the 70-mm still camera presented in Fig. 10 indicate that these two parachutes wound about their suspension lines, decreasing the inflated diameter and thus lowering the drag.

Presented in Fig. 11 is the variation of steady-state drag coefficient as a function of Mach number for two NBB parachutes. The data agreement shown is indicative of the uniform construction of the test parachutes.

Figure 12 shows the steady-state drag-to-weight advantage of Fiber B, and Fig. 8 shows the corresponding volume reduction that can be achieved by substituting Fiber B material for nylon material in parachutes. An increase of 76 percent in drag-to-weight ratio with a 63-percent volume reduction and a 48-percent weight reduction can be realized with Fiber B-constructed parachutes compared to nylon-constructed parachutes.

4.2 PARACHUTE DYNAMIC CHARACTERISTICS

Typical deployment drag time traces of the five parachute configurations at a deployment Mach number of 0.8 and a dynamic pressure of 350 psf are presented in Fig. 13. The traces show the relative time for deployment as referenced to the time of squib ignition and indicate the associated dynamics during deployment. The snatch load occurs at the full extension of the riser and suspension lines, and the opening shock load occurs at the inflation of the chute. An original concern about parachute deployment was that parachutes constructed with Fiber B would not absorb the opening shock load as well as those made of nylon material. Because Fiber B material has a smaller elongation-to-break ratio than nylon material, the ability to absorb opening shock energy by elongation is less for Fiber B than for nylon. The opening shock loads obtained from the oscillograph (see Table 2) for the parachutes constructed of nylon material and for

those constructed of Fiber B material are approximately the same, however, indicating equal shock load energy absorption.

The traces in Fig. 13 show a shorter damping time for the deployment drag dynamics for the parachutes constructed of Fiber B material than for those constructed of nylon material.

The post-deployment parachute drag dynamic characteristics (approximately 2 sec after deployment) of each parachute were determined from the statistical analysis program which reduces the drag data recorded by a high-speed digital data recording system at a sampling rate of 2000 samples per second and which calculates the drag distribution parameters of kurtosis, skewness, standard deviation, and the average drag coefficient. The parameters are tabulated on the dynamic drag coefficient distribution sample plot presented in Fig. 14 and summarized in Table 3. Also presented is the 95-percent confidence level interval, which can be interpreted as representing a quantitative measurement of drag dynamics at a 95-percent confidence level. The drag dynamics of the test parachutes can be compared by each parachute's relative dynamic parameter, which is found by dividing the 95-percent confidence interval, expressed as the drag coefficient interval, by the average drag coefficient. These values are also tabulated in Table 3. The significance of the relative dynamic parameter can be shown by reviewing the drag dynamic characteristics of a parachute having a Gaussian-type drag distribution when values of zero, unity, and two are assigned to the relative dynamic parameter. A value of zero implies no dynamics; a value of unity implies that the magnitude of the dynamics about the average drag coefficient is equal to 50 percent of the average drag coefficient; a value of two implies that the magnitude of the dynamics about the average is equal to 100 percent of the average drag coefficient. The deviation of the skewness parameter from zero indicates that the statistical distribution is not symmetrical about the average drag coefficient. Positive values of this parameter indicate higher dynamics above the average value, and likewise, negative values indicate lower dynamics than the average value. A value of three for the kurtosis parameter represents a typical Gaussian-type statistical distribution.

As shown in Table 3 and Fig. 15, the relative dynamic parameter and the standard deviation of parachutes partially or wholly constructed of Fiber B material are less than those of the all-nylon parachute. The BBB and NBB parachutes which have Fiber B-constructed radials and canopy ribbons exhibit the least post-deployment drag dynamics and the smallest standard deviations. This indicates that most of the drag dynamics can be eliminated by constructing parachute canopies with Fiber B material in place of nylon material. Statistical analysis data of the BNN1 and NNN4 parachutes is not comparable with the rest of the data because these parachutes collapsed during data acquisition.

Analysis of the motion pictures shows there are no trends evident in winding of the riser lines or suspension lines or in translational movement among the various parachutes tested. Some chutes did collapse after the suspension lines and riser lines had wound, but this characteristic was not limited to any parachute type and could be eliminated by the use of a swivel. The motion pictures show that the NNN2, NNN3, NBB2, and BBB1 parachutes wound about the riser lines. The parachutes that collapsed because of winding were the NNN4, BNN1, and NBB1 parachutes. Parachutes suffering damage during deployment were the NNN1, which wound about the riser lines and suspension lines after creating two holes in the canopy, and the BBB4, which remained stable after breaking one suspension line.

5.0 CONCLUDING REMARKS

Tests were conducted to determine the deployment and inflation characteristics, dynamics, and drag of parachutes constructed with a new textile material, Fiber B. The tests were conducted at Mach numbers from 0.6 to 1.3 and dynamic pressures from 200 to 530 psf. The following observations summarize the results.

1. An increase of 76 percent in drag-to-weight ratio with 63-percent volume reduction and 48-percent weight reduction can be achieved with Fiber B-constructed parachutes compared to nylon-constructed parachutes.
2. Fiber B-constructed parachutes absorbed opening shock loads as well as all nylon-constructed parachutes.
3. The steady-state drag of the all-Fiber B parachute increased with increasing dynamic pressure, whereas the all-nylon parachute steady-state drag was constant with increasing dynamic pressure.
4. Parachutes partially or wholly composed of Fiber B material exhibited less steady-state drag than the all-nylon-constructed parachutes at the same dynamic pressures.
5. The damping time for the deployment drag dynamics was shorter for the Fiber B-constructed parachutes compared to the all-nylon constructed parachutes.
6. Post-deployment drag dynamics for Fiber B-constructed parachutes were lower compared to all-nylon-constructed parachutes. The least drag dynamics occurred for those parachutes having radials and canopy ribbons constructed of Fiber B material.

REFERENCES

1. Test Facilities Handbook (Ninth Edition). "Propulsion Wind Tunnel Facility, Vol. 4." Arnold Engineering Development Center, July 1971.
2. Galigher, Lawrence L. "Aerodynamic Characteristics of Ballutes and Disk-Gap-Band Parachutes at Mach Numbers from 1.8 to 3.7." AEDC-TR-69-245 (AD861437), November 1969.

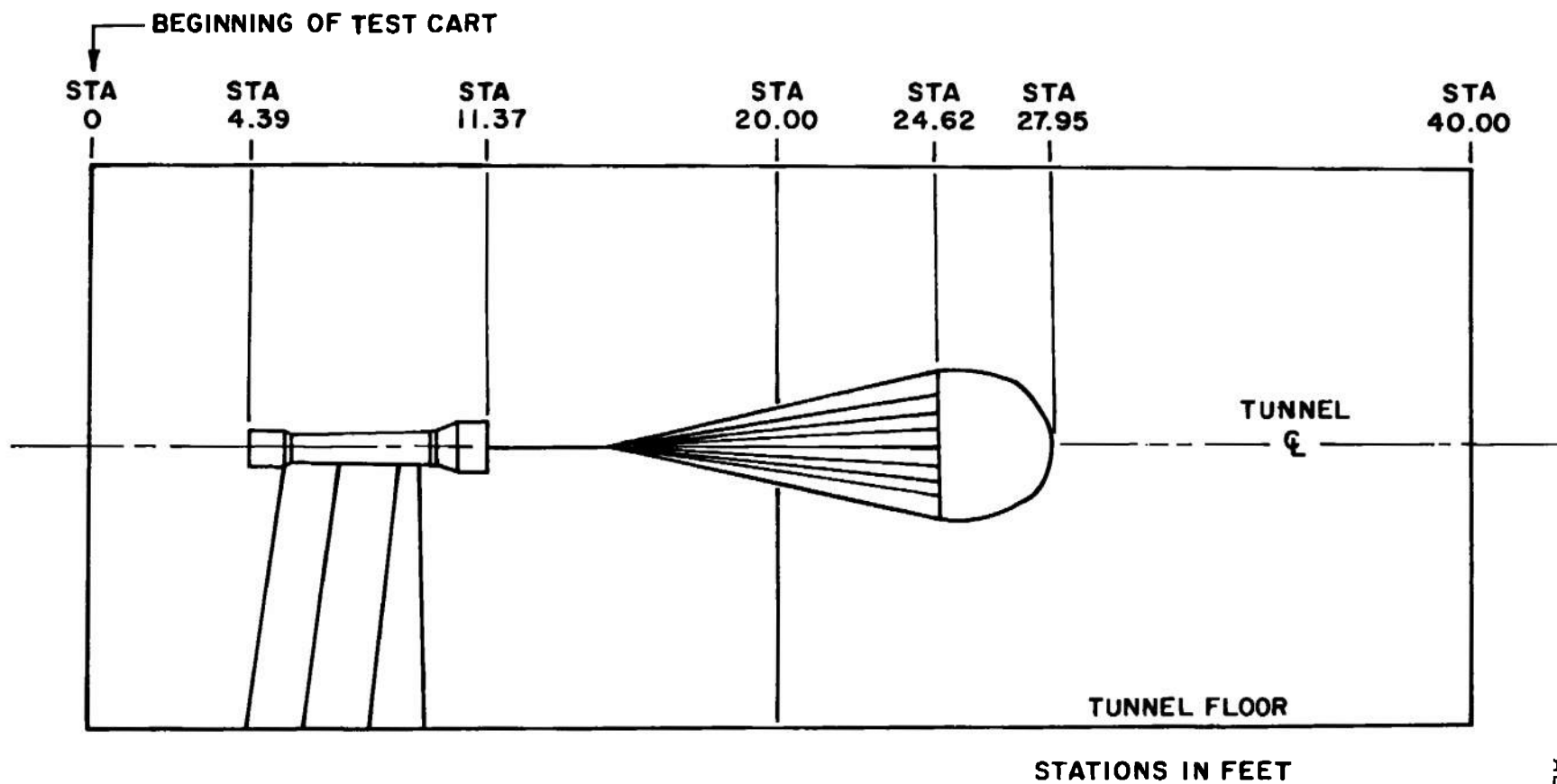


Figure 1. Model location in test section.

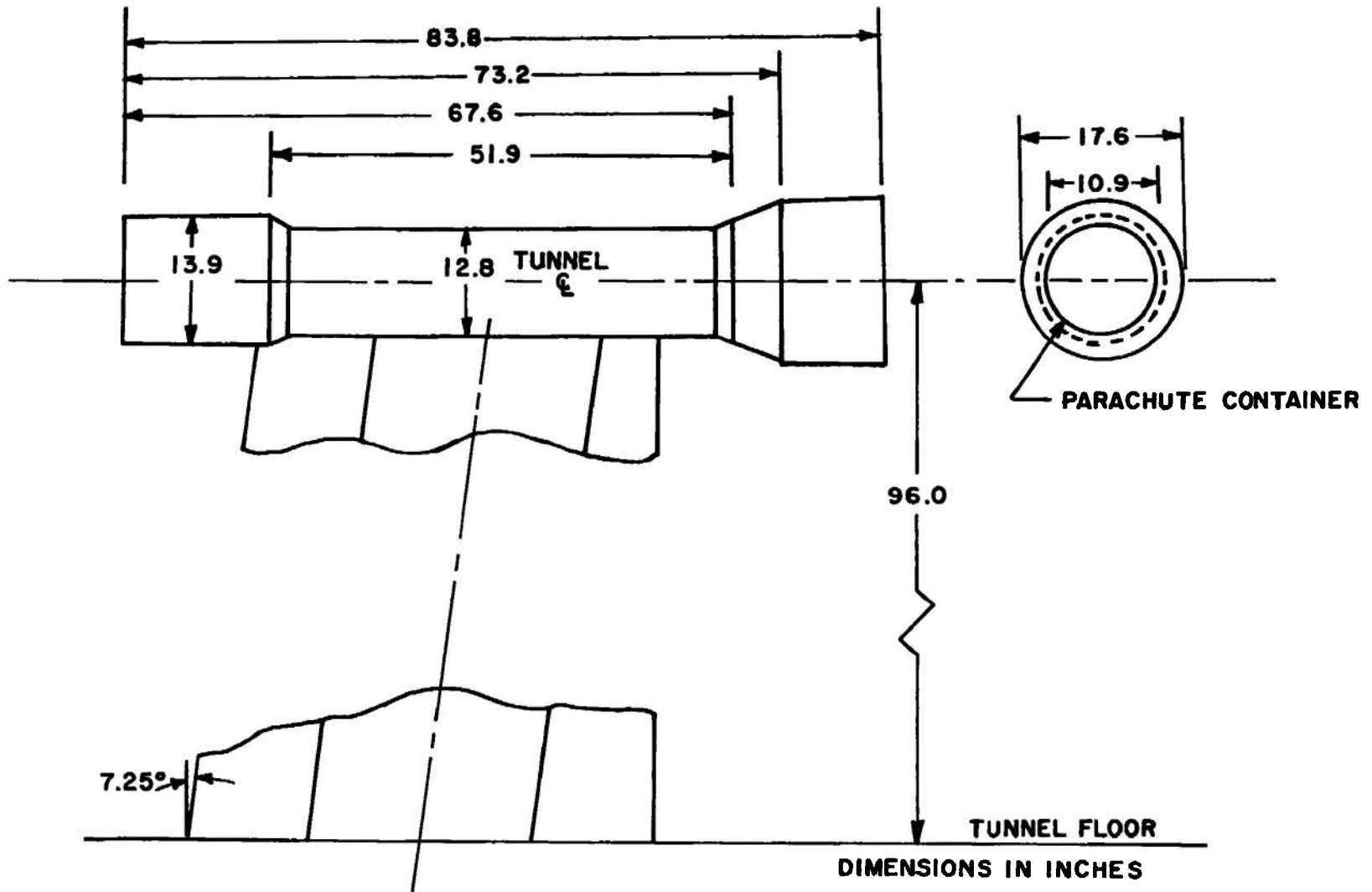


Figure 2. Sketch of model forebody.

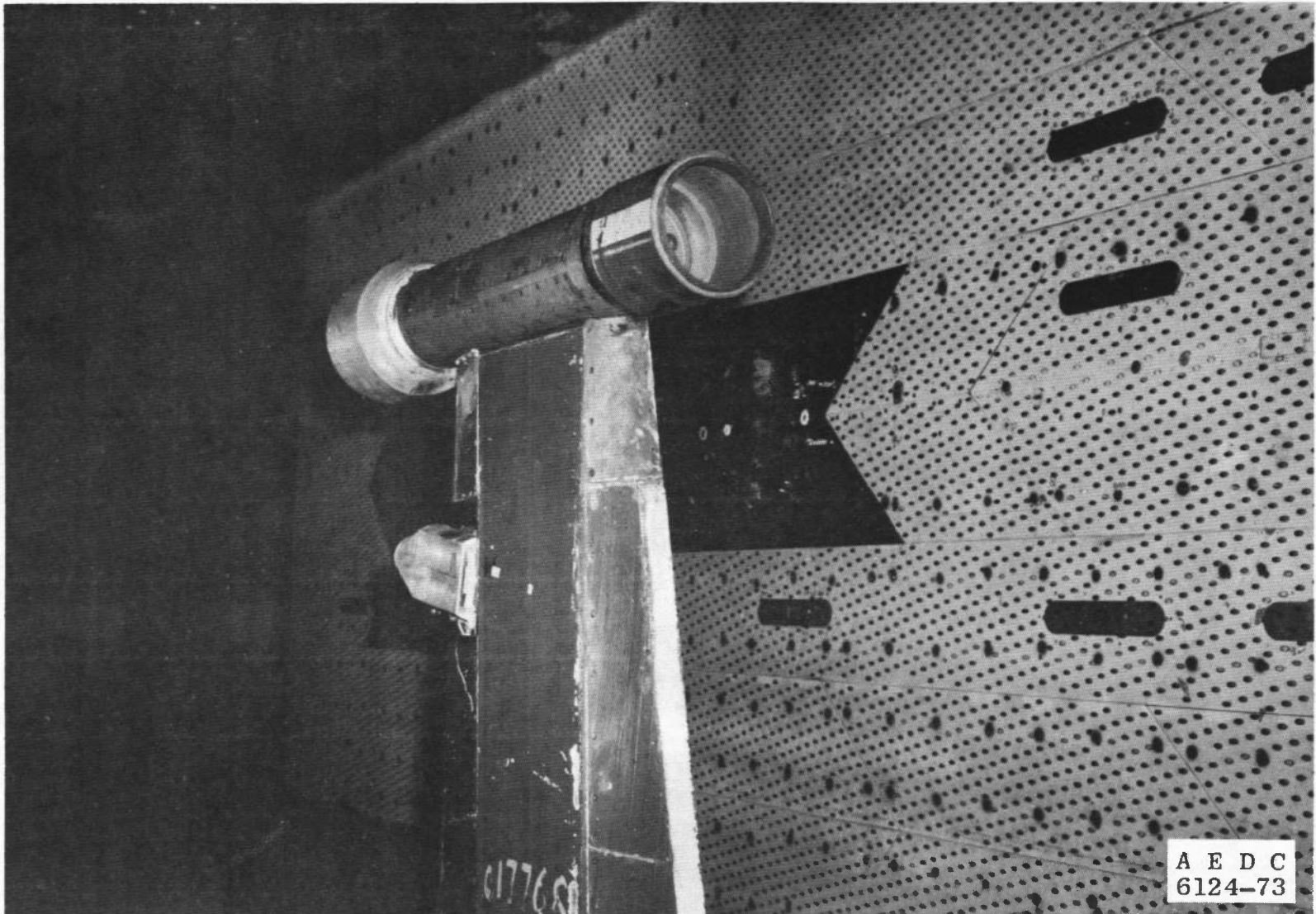


Figure 3. Installation of model forebody in test section.

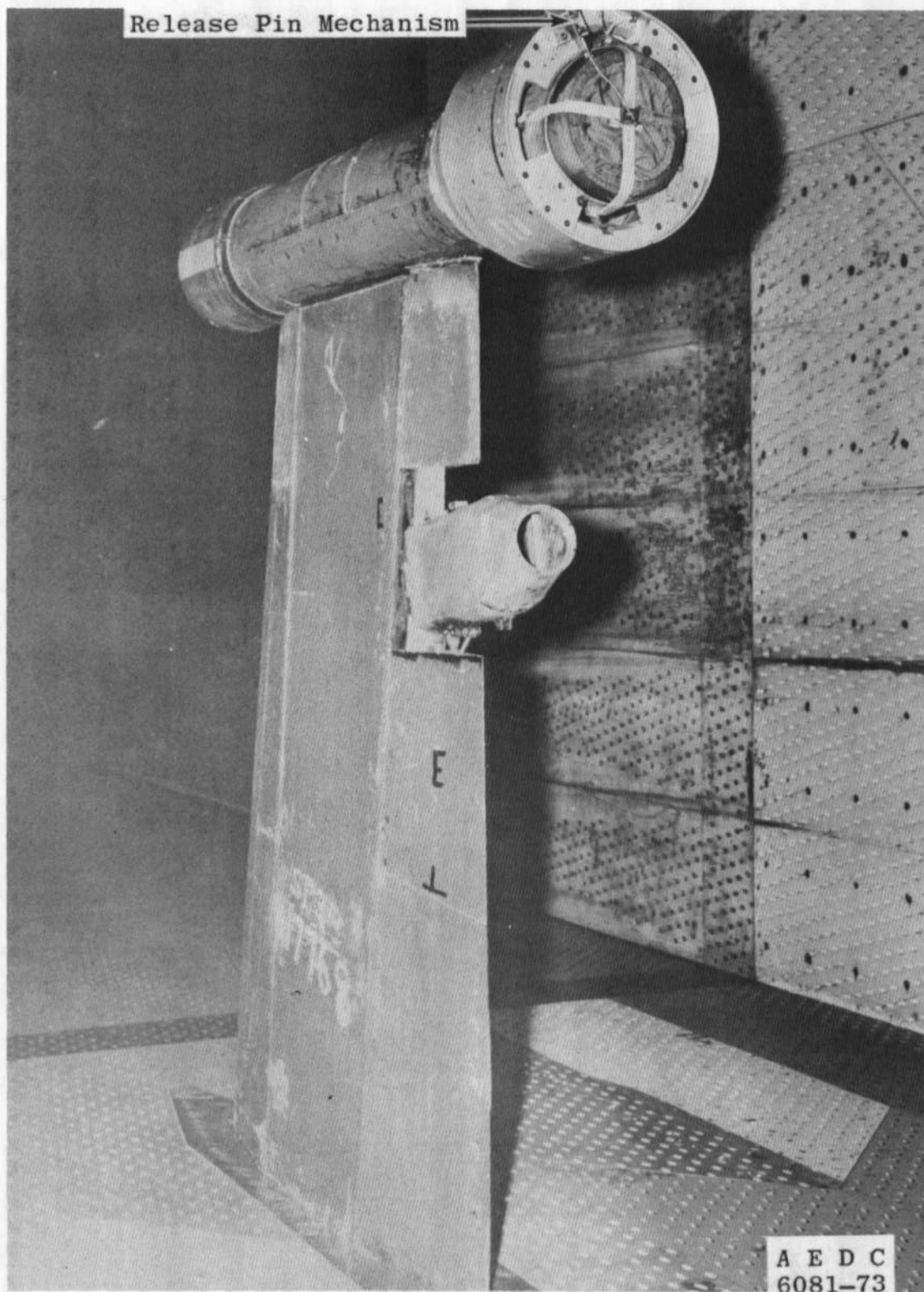
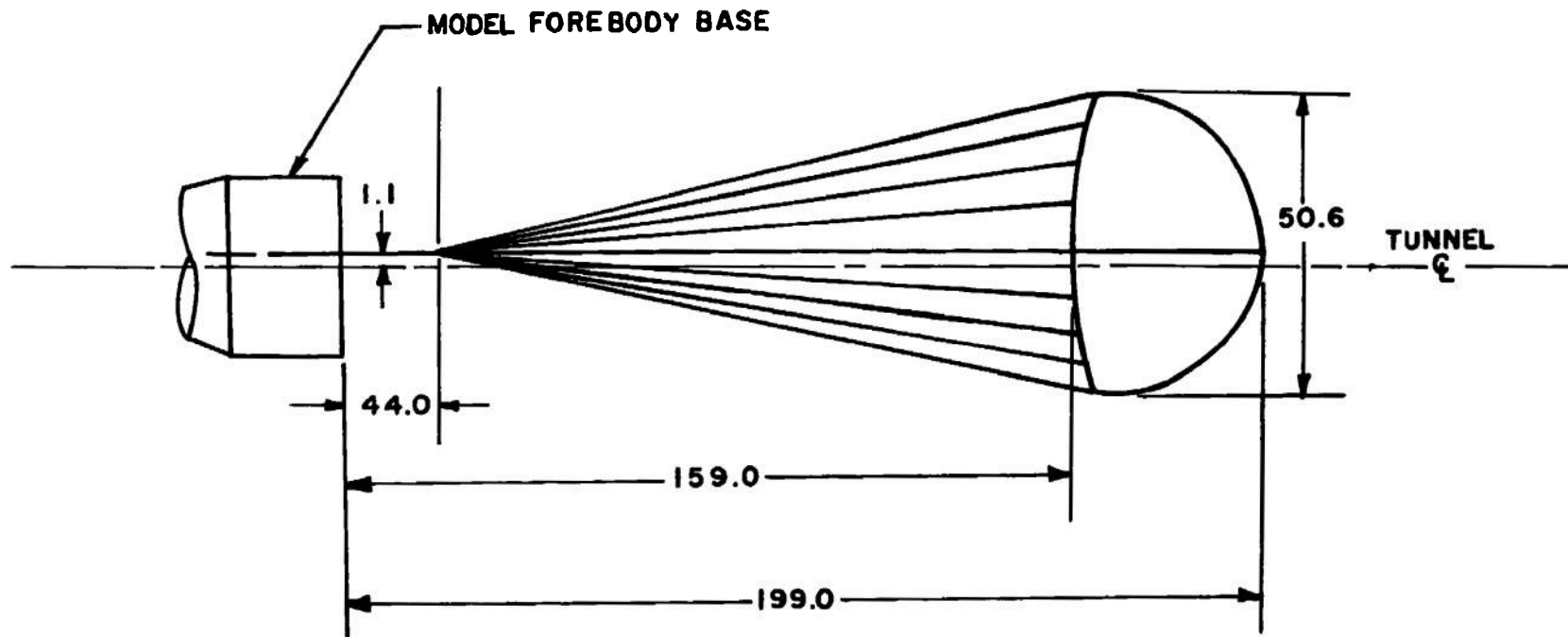


Figure 4. Parachute installation.

AEDC-TR-73-184



DIMENSIONS IN INCHES

TUNNEL FLOOR

Figure 6. Sketch of test parachute.

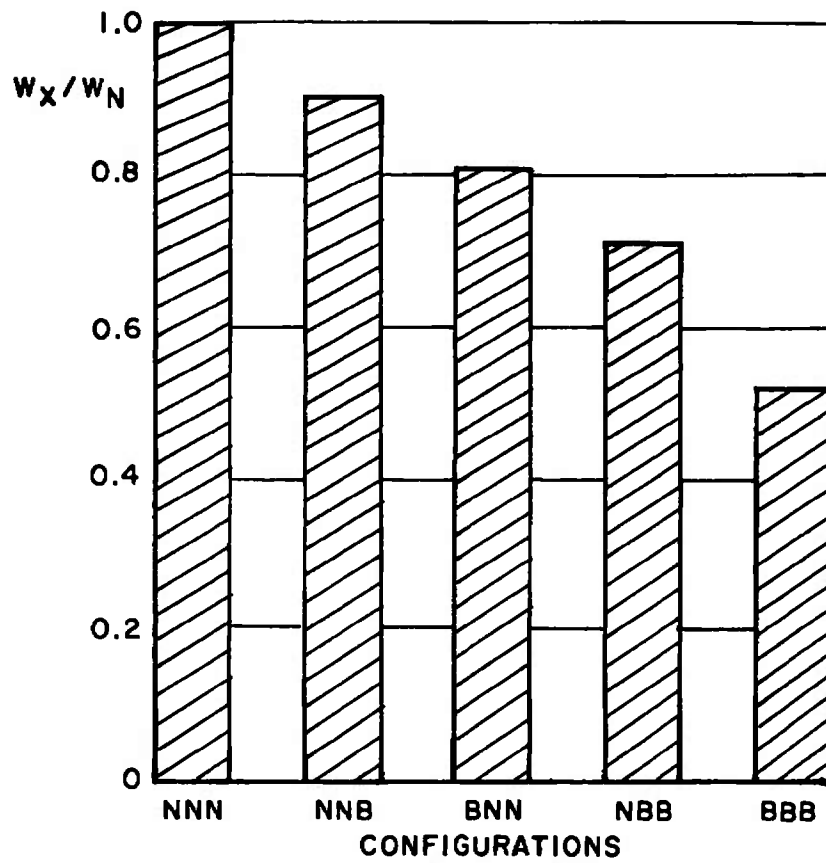


Figure 7. Weight comparison of parachute configurations.

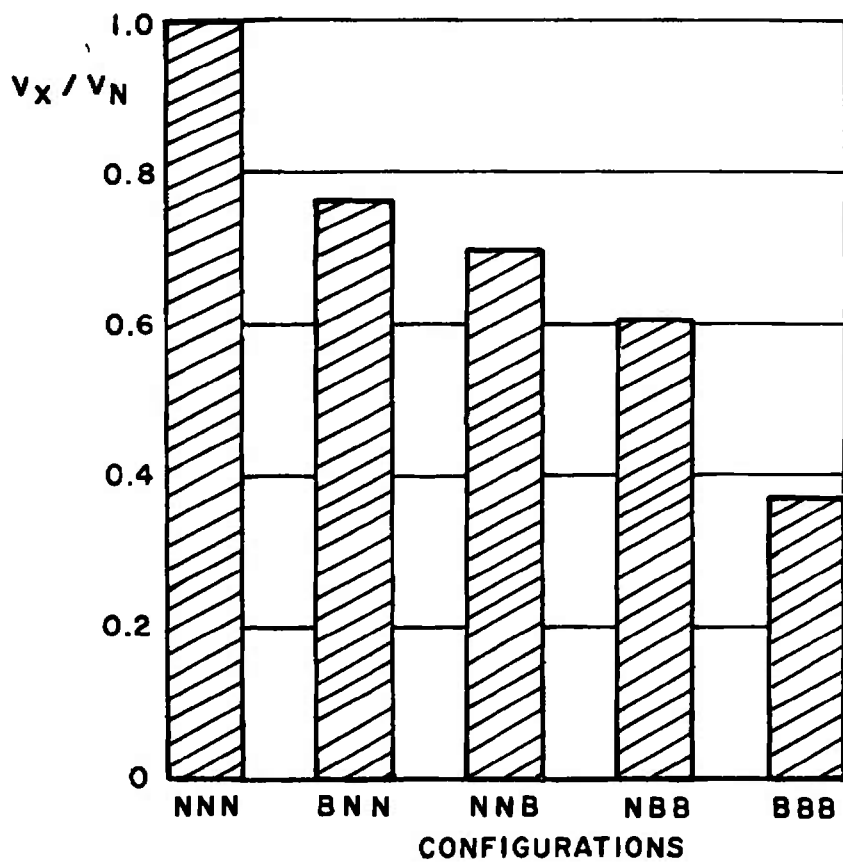


Figure 8. Volume comparison of parachute configurations.

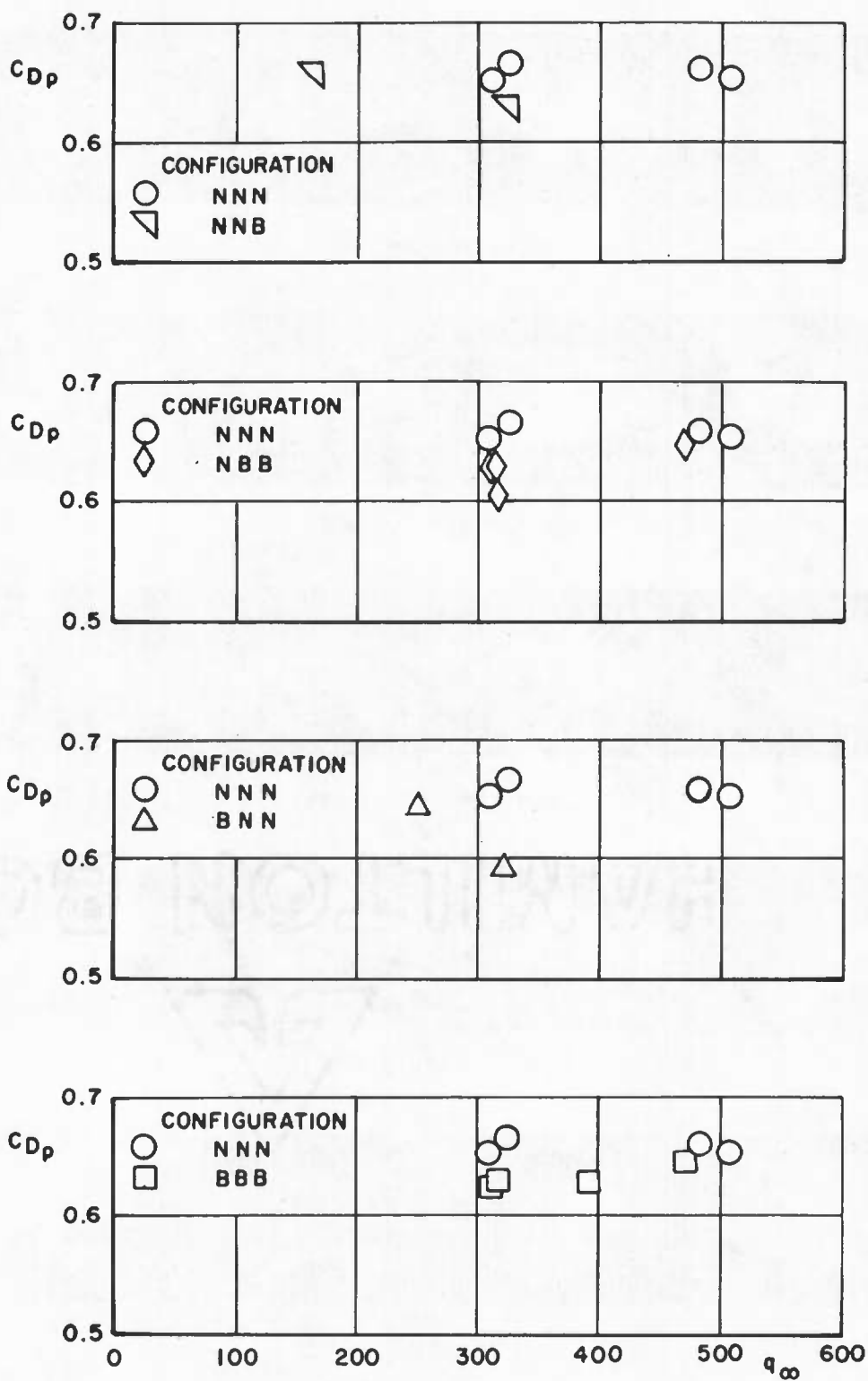
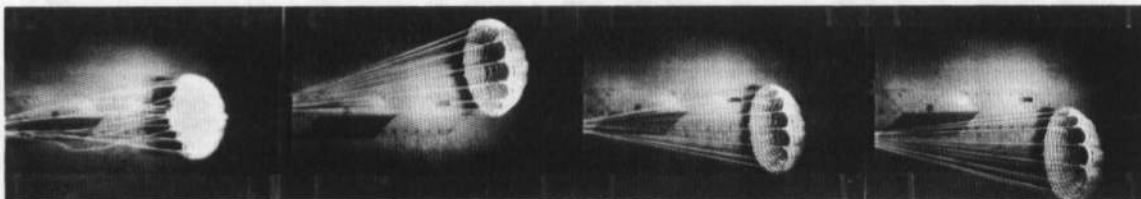
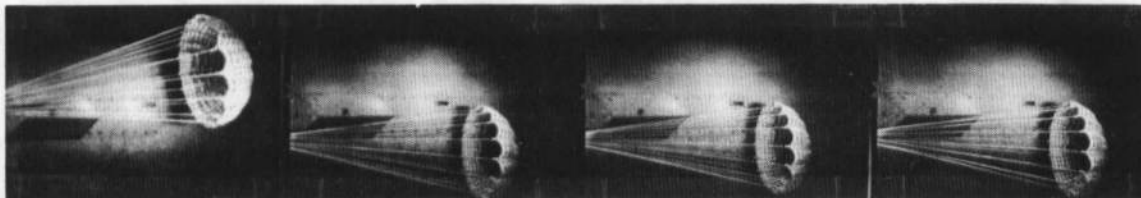


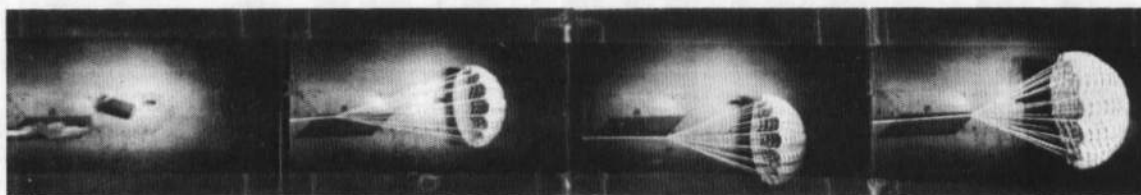
Figure 9. Variation of drag coefficient with dynamic pressure, $M_\infty = 0.8$.



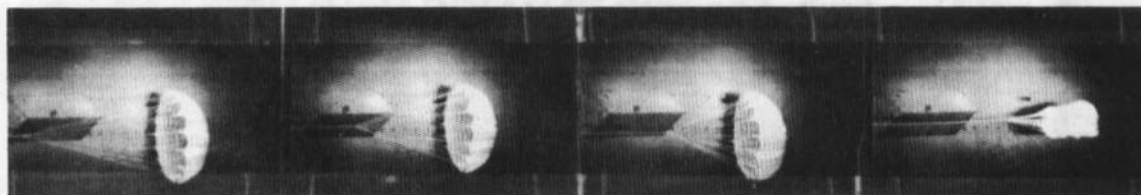
CONFIGURATION NNN2



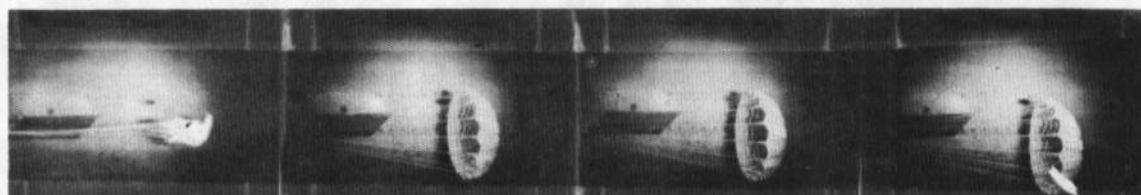
CONFIGURATION NNB1



CONFIGURATION NBB1



CONFIGURATION BNN1



CONFIGURATION BBB1

Figure 10. Typical photographs of deployment and inflation of the parachute configurations, $M_\infty = 0.8$, $q_\infty = 350$ psf.

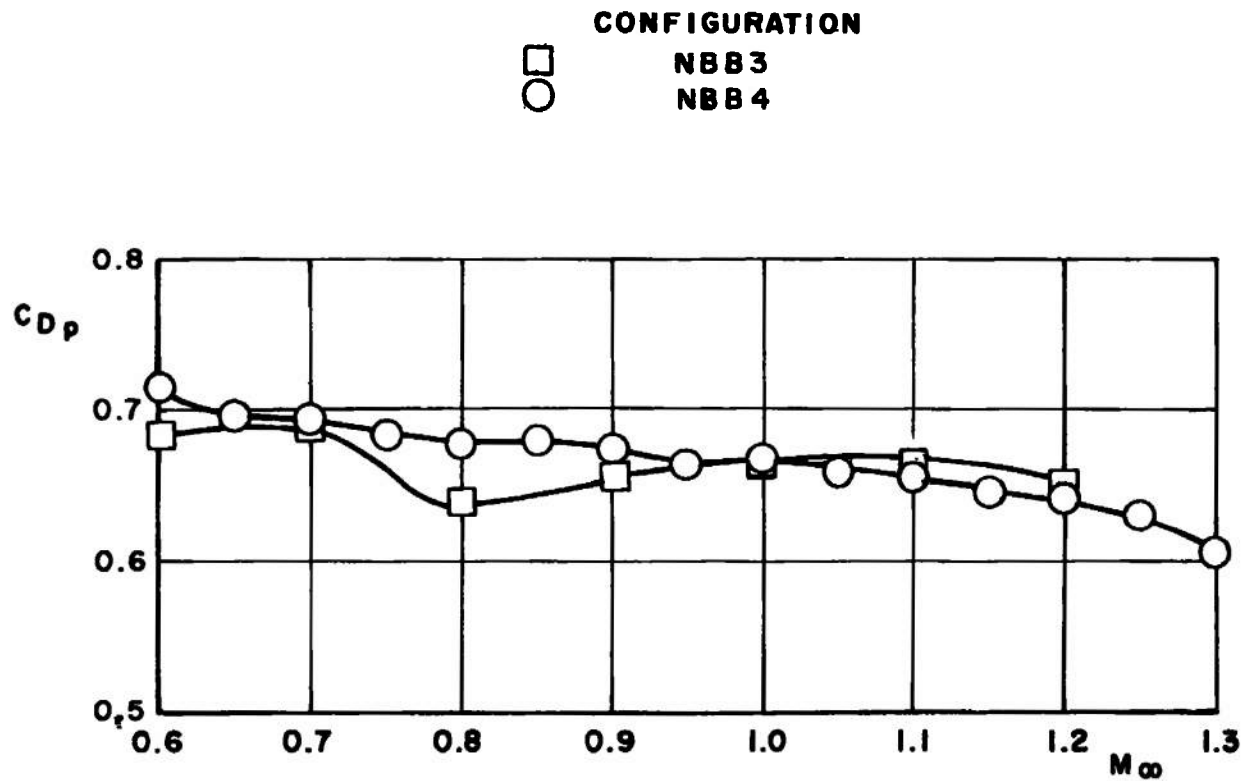


Figure 11. Variation of parachute drag coefficient with Mach number, $q_\infty = 200$ psf.

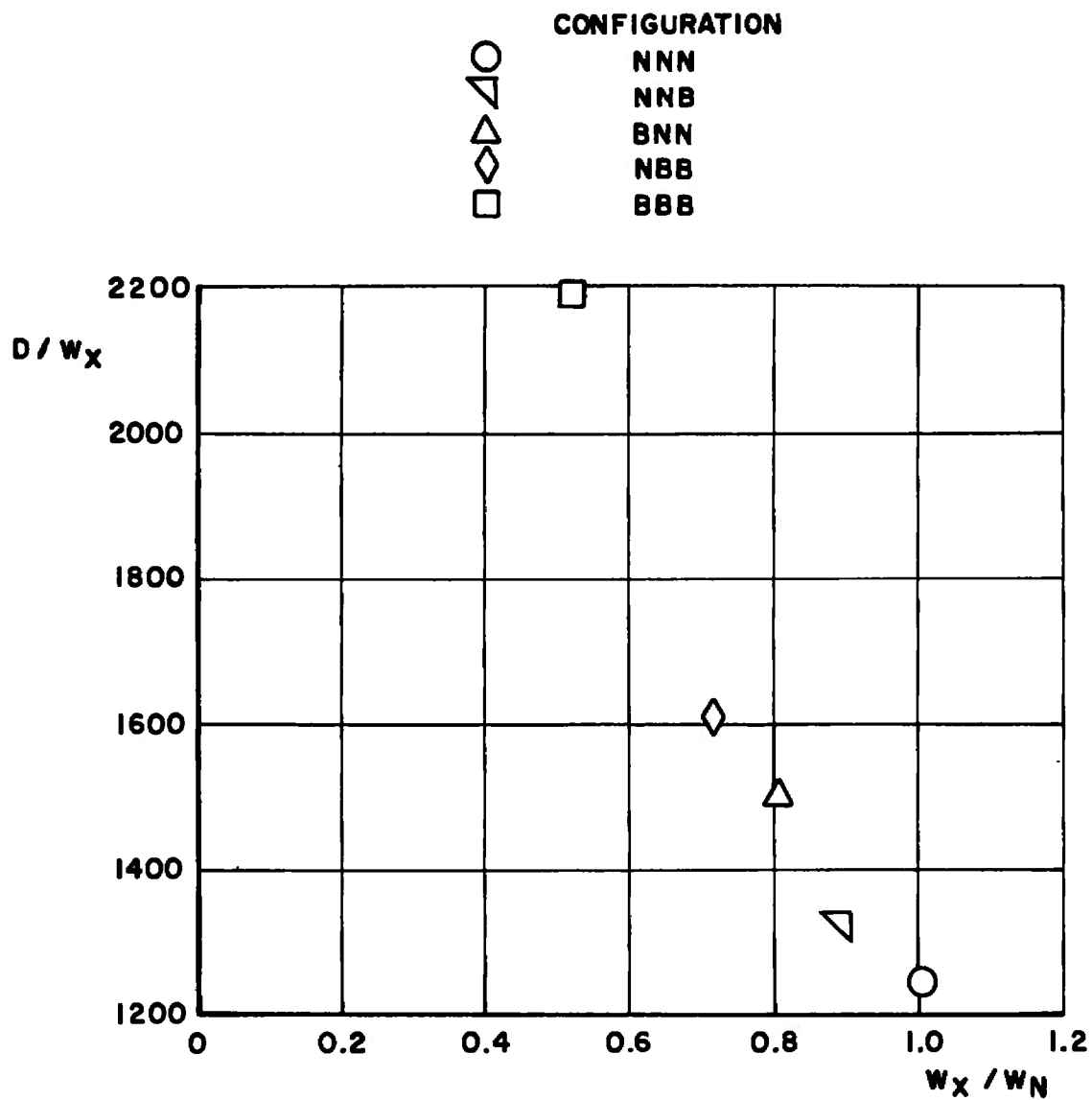


Figure 12. Drag-to-weight ratio of various configurations, $M_\infty = 0.8$, $q_\infty = 350$ psf.

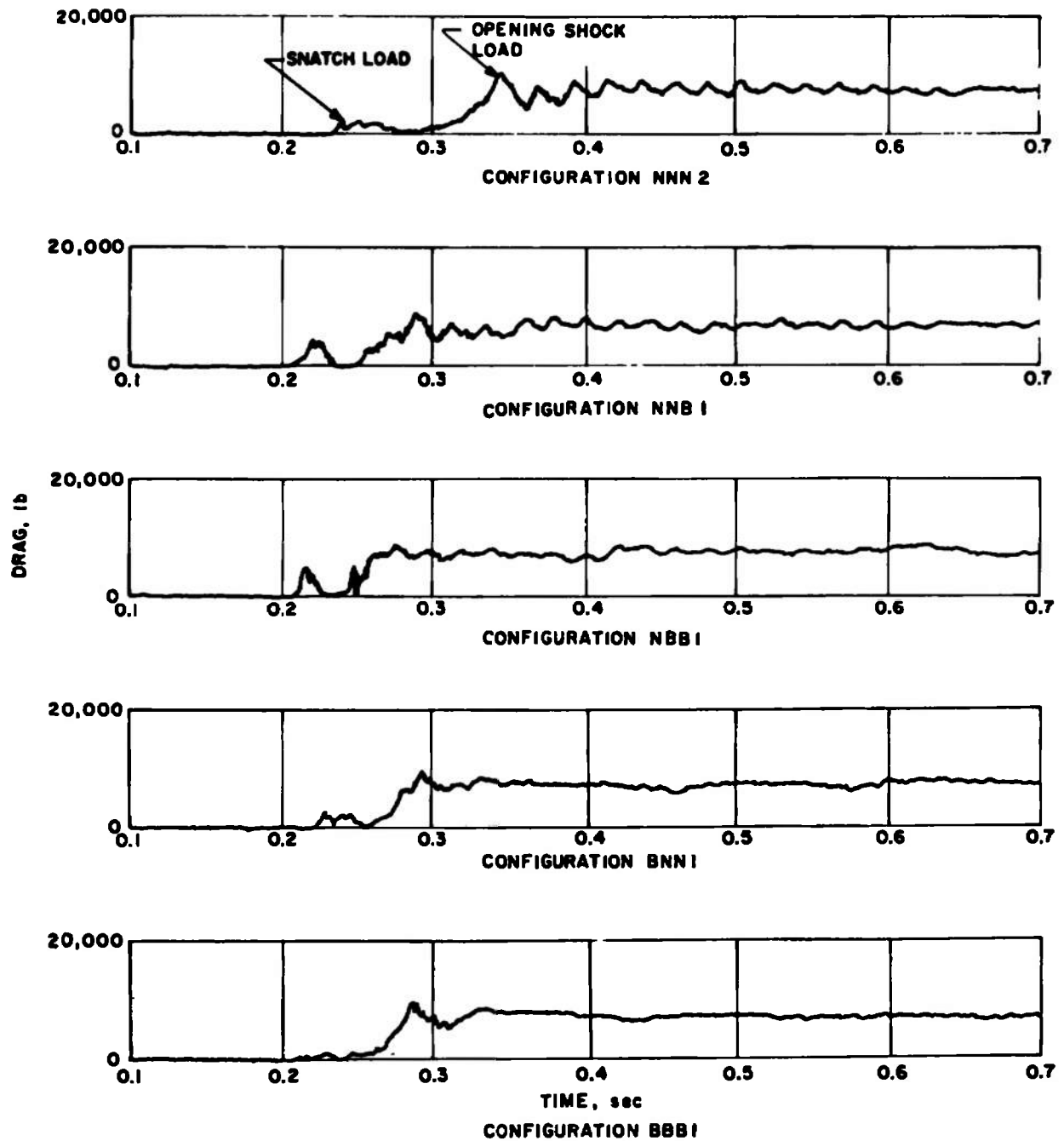


Figure 13. Deployment characteristics of various configurations, $M_\infty = 0.8$, $q_\infty = 350$ psf.

C_{Dp}	σ	SKEWNESS	KURTOSIS	$(N_i)_{MAX}$	N	RDP
0.645	0.012	0.004	2.976	1247	4096	0.111

$$C_{Dp} = 0.645 \begin{matrix} + 0.048 \\ - 0.023 \end{matrix} \quad (95\% \text{ CONFIDENCE LEVEL})$$

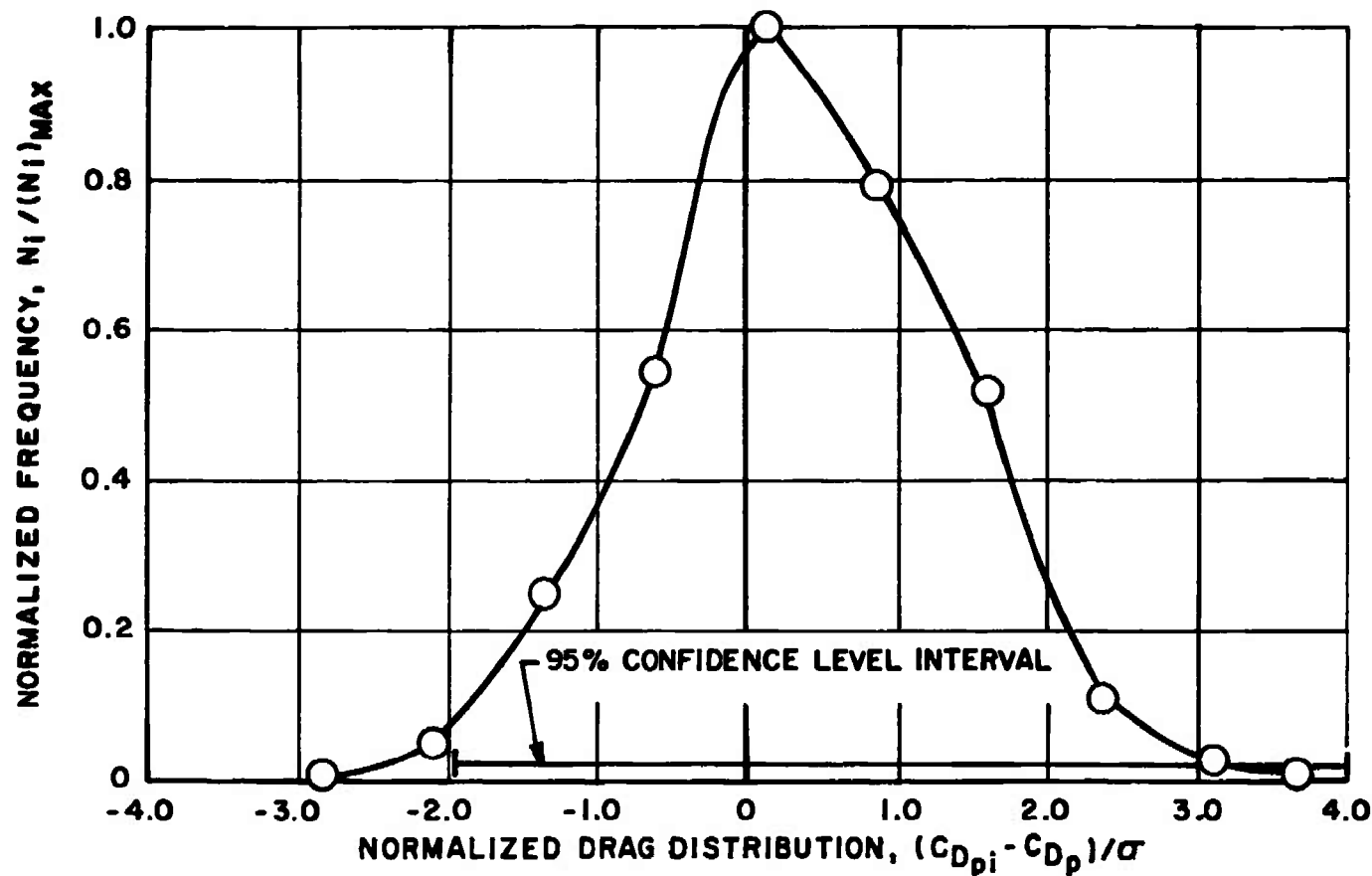


Figure 14. Typical distribution plot of the parachute dynamic drag characteristics, $M_\infty = 0.8$, $q_\infty = 440$ psf, configuration BBB3.

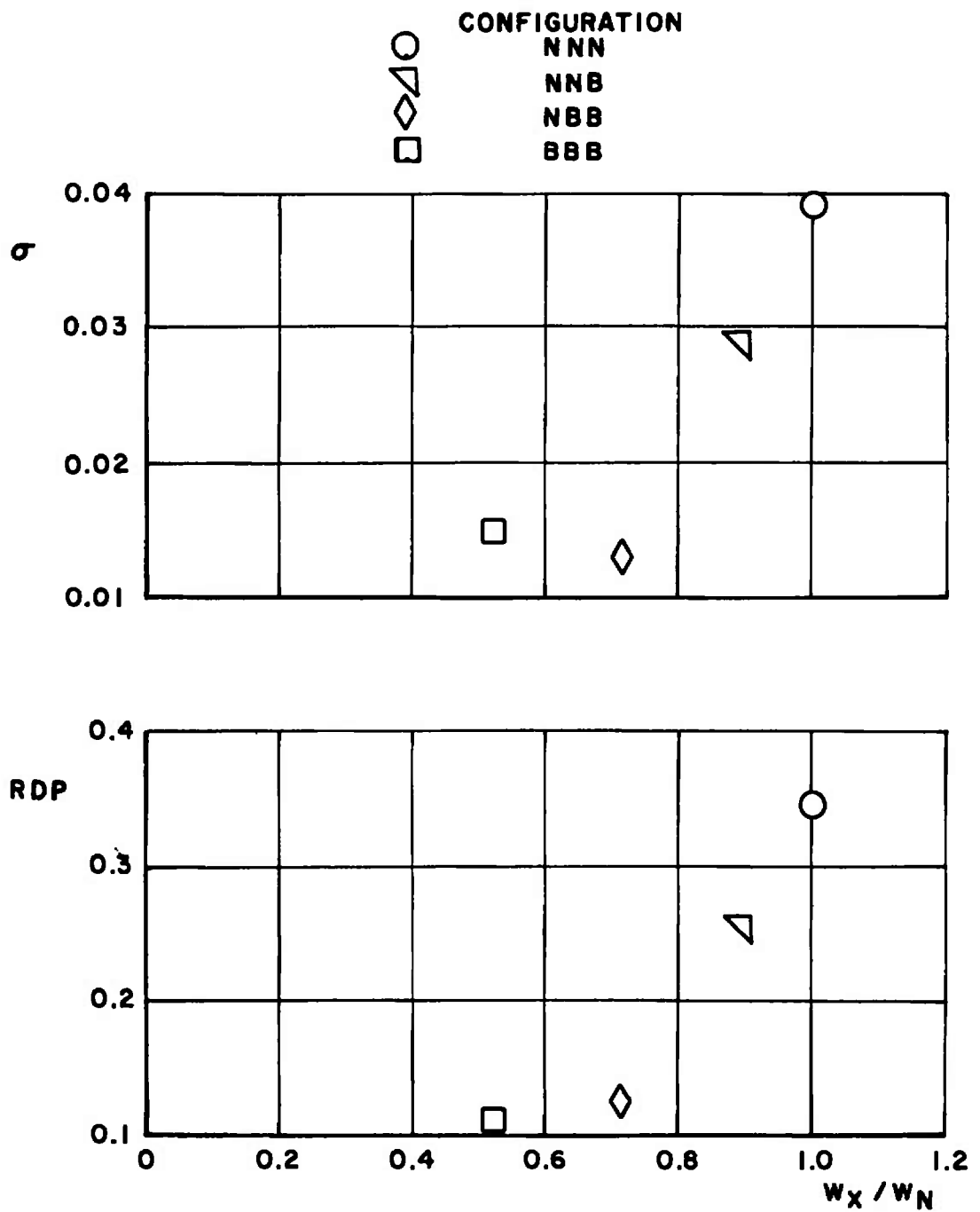


Figure 15. Relative dynamic parameter and standard deviation for various configurations, $M_\infty = 0.8$, $q_\infty = 350$ psf.

Table 1. Parachute Configuration Construction

Parachute Type	Run Numbers	Material Construction		
		Suspension Lines	Radials	Canopy Ribbons
NNN	1 - 4	Nylon	Nylon	Nylon
NNB	1 - 2	Nylon	Nylon	Fiber B
NBB	1 - 4	Nylon	Fiber B	Fiber B
BNN	1 - 2	Fiber B	Nylon	Nylon
BBB	1 - 4	Fiber B	Fiber B	Fiber B

Table 2. Test Summary

Configuration	Nominal Mach Number, M_∞	Nominal Dynamic Pressure, q_∞ , psf	Opening Shock Load, lb
NNN1	0.80	530	11,870
NNN2	0.80	350	10,090
NNN3	0.80	350	9,490
NNN4	0.80	530	14,640
NNB1	0.80	350	8,700
**NNB2	0.57	165	6,130
BNN1	0.80	350	8,900
**BNN2	0.68	239	---
NBB1	0.80	350	8,310
NBB2	0.80	350	8,710
*NBB3	0.66	337	9,890
*NBB4	0.80	530	13,260
BBB1	0.80	350	9,500
BBB2	0.80	350	8,510
BBB3	0.80	440	10,680
BBB4	0.80	530	11,670

*Steady-state data acquired at $M_\infty = 0.6$ to $M_\infty = 1.3$ and $q_\infty = 200$ psf

**Premature deployment

Table 3. Parachute Statistical Analysis Summary

Configuration	Average Drag Coefficient, C_{Dp}	σ , Deviation	Skewness	Kurtosis	N, Total Number Samples	Relative Dynamic Parameter
NNN1	0.625	0.038	0.935	2.445	4096	0.307
NNN2	0.659	0.039	0.588	3.070	4096	0.347
NNN4	0.649	0.019	-0.317	2.666	4096	0.173
NNB1	0.656	0.029	-0.470	2.845	4096	0.257
BNN1	0.660	0.029	0.419	2.979	4096	0.259
NBB2	0.629	0.013	-0.320	2.994	4096	0.126
BBB1	0.627	0.015	0.474	2.807	4096	0.138
BBB2	0.624	0.014	0.020	3.185	4096	0.136
BBB3	0.645	0.012	0.004	2.976	4096	0.111

NOMENCLATURE

C_{D_p}	Parachute drag coefficient, $D/q_\infty S$
$C_{D_{pi}}$	Mean parachute drag coefficient value of each cell in the statistical analysis program, $D/q_\infty S$
D	Drag force, lb
M_∞	Free-stream Mach number
N	Total number of drag coefficient data samples used in the statistical analysis program
N_i	Number of drag coefficient data samples in each cell of the statistical analysis program
$(N_i)_{MAX}$	Maximum number of drag coefficient samples in any cell of the statistical analysis program
q_∞	Free-stream dynamic pressure, psf
S	Parachute reference area, 32.169 sq ft
V_N	Volume of nylon parachute configuration
V_X	Volume of any parachute configuration
W_N	Weight of nylon parachute configuration
W_X	Weight of any parachute configuration
X/D	Distance in forebody diameters ($D = 17.6$ in.) from model base to leading edge of parachute skirt, 9.024
σ	Standard deviation of the distribution of drag coefficient data determined from the statistical analysis program
Relative Dynamic Parameter, RDP	Ratio of the 95-percent confidence level interval, expressed as drag coefficient interval, of a distribution of drag coefficient data to the average drag coefficient value as determined from the statistical analysis program